Proceedings World Geothermal Congress 2020+1
Reykjavik, Iceland, April - October 2021

Preliminary Results of the Seismicity Induced During the Stimulation of the Vendenheim Enhanced Geothermal System (France)

Emmanuel Gaucher[1], Marine Jolivet[2], Mariane Peter-Borie[3]

[1] KIT, Institute of Applied Geosciences, Division of Geothermal Research, Kaiserstraße 12, D-76131 Karlsruhe, Germany

[2] Fonroche, Technopole Hélioparc, 2 avenue Pierre Angot, F-64053 Pau, France

[3] BRGM, 3 avenue Claude Guillemin, F-45060 Orléans, France

Corresponding author: emmanuel.gaucher@kit.edu

Keywords: DEEPEGS, EGS, Stimulation, Induced seismicity, Monitoring, Upper Rhine Graben

ABSTRACT

The European H2020 DEEPEGS project aims at demonstrating that enhanced geothermal systems can be developed and produce energy efficiently in different geological and geographical contexts across Europe. Two main demonstrators are involved, one located in Iceland, in the Reykjanes peninsula and one located in France, at Vendenheim, in the Upper Rhine Graben. One of the project goal is to apply passive seismic monitoring to mitigate induced seismicity and to assess the geothermal reservoir development.

We focus on the Vendenheim site, which is located in the northern suburb of Strasbourg (France). In 2018-2019, a well doublet was drilled and targets a fault in the granitic basement at ~4.6 km depth, where temperatures above 200°C were measured. The initial injectivity/productivity of the wells was too small and required stimulations to enhance the geothermal system and produce energy under economic conditions. These operations were monitored using a permanent seismic monitoring network completed by a temporary network. In total, nine stations recorded the seismicity induced by the operations. We present here preliminary results associated with the seismicity recorded during the hydraulic stimulation of the well VDH-GT2.

1. INTRODUCTION

The DEEPEGS project is a project of the European Union's Horizon 2020 research and innovation programme (grant agreement No. 690771), which started end of 2015. It gathers ten partners, among which five energy companies, whose goal is to demonstrate the capabilities of enhanced geothermal systems (EGS) to deliver competitive renewable energy across Europe. Various stimulation techniques and innovative technologies are applied, tested and assessed to establish a "tool box" applicable in different geological conditions. Two main geothermal fields are involved: the Reykjanes field (Iceland) (Friðleifsson *et al.* 2017) in a super-critical volcanic context and the Vendenheim field (France), a lower enthalpy system in the Upper Rhine Graben context.

Per definition, EGS require well stimulation in order to develop an economically viable reservoir enabling geothermal fluid production at high temperature and high rates. The purpose of the stimulation is to increase the connectivity between the wells – injector(s) or producer(s) – and the rock formation, and to increase the permeability of usually tight geological formations. Various stimulation methods may be applied at one site (chemical, thermal, hydraulic), however, the economical field development must not compromise the environment nor the society for sustainable use of this renewable energy. With this regard, monitoring of induced seismicity is one aspect to consider. Indeed, geothermal well stimulation is often accompanied by induced seismicity (Majer *et al.* 2007; e.g. Evans *et al.* 2012; Zang *et al.* 2014). This reflects the mechanical response of the rock, which can occur far from the well, to the forced-fluid circulation. Hence, induced seismicity is also a unique tool to characterize the geometry of the effectively developed reservoir. Consequently, seismic monitoring at geothermal fields must satisfy two objectives: seismic hazard mitigation and reservoir imaging.

In the following, we present preliminary results associated with the seismicity induced during the stimulation of the VDH-GT2 well at Vendenheim, but we first start by describing the field context.

2. VENDENHEIM CONTEXT

2.1 Geological Settings

The Vendenheim site is located in the Upper Rhine Graben (URG) (Figure 1), which is part of the European Cenozoic Rift System (ECRIS) (Ziegler 1992; Dèzes, Schmid and Ziegler 2004). This approximatively 300 km long and 40 km wide rift is bounded on the French side by the Vosges mountains and on the German side by the Black Forest. The URG is structured by a complex set of discontinuities (Schumacher 2002; Meixner *et al.* 2016). The targeted fault zone in the basement of Vendenheim have been probably created during Permo-Carboniferous times and submitted to repeatedly changing stress field leading to its reactivation. The Variscan orogeny (Paleozoic times) structured the basement of the URG. Three main faulting directions have been identified or suspected in the basement: major NE to ENE striking structures, sinistral NNE-striking fault zone and N to NNW-striking Riedel shears probably subordinated to the NNE-striking faulting. At large scale, Vendenheim is located in the vicinity of the junction between the dextrally sheared Lalaye-Lubine-Baden-Baden fault (LB) and the major sinistral NNE faulting zone. In Cenozoic, rifting occurred and led to the current horst and graben structure typical of the central part of the basin.

The Vendenheim well doublet targets a N10°E-striking and 82°W-dipping fault in the granitic basement. The fault core is located approximately 100 m deeper than the top of the basement, which is approximately at 4.1 km depth TVD MSL. This main fault was created in Paleozoic by sinistral shearing and then normal faulting took place during Cenozoic times. A second fault with relatively

similar direction and dipping exist to the west but merge with the first one about 10 km north from Vendenheim site. Close to the branching point, a complex sub-fault network develops in the sedimentary part comprising secondary antithetic faults.

The URG is assumed to be globally an Andersonian system, i.e. with the vertical stress a principal stress direction. The faulting regime varies from normal faulting (mostly in the sedimentary part) to strike-slip regime. Interpretations of fault-plane solutions also reveal a change in faulting regime in the URG (e.g. Plenefisch and Bonjer 1997): the northern part of the URG is characterized by an extensional stress state and active normal faulting, but in the seismically more active southern part, strike-slip faulting with secondary normal faulting prevails (Meixner *et al.* 2016). Permutation between σ_1 and σ_2 are measured, in particular, in the basement of Soultz-sous-Forêts (Cornet, Bérard and Bourouis 2007). The main horizontal stress is roughly oriented NW–SE with local variations from N130°E to N180°E (Cornet *et al.* 2007; Dorbath *et al.* 2010; Meixner *et al.* 2016). The main horizontal stress is supposed closer to N130°E in the northern part of the URG and to N145° to N160° in the southern part/northern Switzerland (Delouis *et al.* 1993; Plenefisch and Bonjer 1997).

A first estimate of the stress state in the sedimentary layers of Vendenheim was conducted from borehole breakouts and image logs in the VDH-GT1 well. Under normal regime, as often observed in the sedimentary part of the URG, the major horizontal stress is estimated to be oriented between N150°E-N170°E. No stress state estimate could be conducted in the basement.

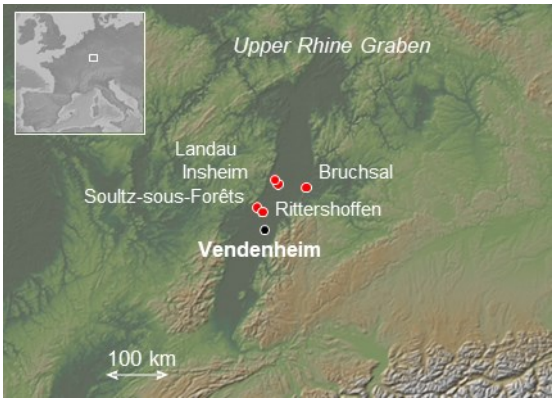

Figure 1: Location of the Vendenheim geothermal site (black point) in the Upper Rhine Graben. The nearby deep geothermal fields are indicated (red points).

2.2 Field Development

Vendenheim is located about 10 km to the north of Strasbourg, or 35 km south of the Soultz-sous-Forêts and Rittershoffen deep geothermal sites. The geothermal plant operated by Fonroche is located in the newly developed "Ecoparc Rhénan" and should deliver 5 MWe and 15 MWth. In February 2018, drilling of the first well, VDH-GT1, was carried out. This well reached 4516 m depth (TVD MSL) and its open hole section is 1700 m long in the upper granitic basement. At depth, temperature larger than 210°C was measured, which makes this well the hottest well of the URG. VDH-GT1 well was tested in March 2018. In August 2018, took place the drilling of the second well, VDH-GT2. In May 2019, testing was done and showed the necessity to perform stimulation to improve the well-reservoir transmissivity. The plan was to conduct a hydraulic stimulation first and then a thermal stimulation. This work focuses on the hydraulic stimulation since the thermal stimulation is on-going when we write this paper.

3. PASSIVE SEISMIC MONITORING

3.1 Seismic Network

For the development of the Vendenheim geothermal field, Fonroche deployed five permanent seismological stations, VDH2 to VDH6 connected in real time to the monitoring system (Figure 2). This permanent network started recording permanently from January 2017, 6 months prior to any drilling on site, as required by the French local authorities. The stations are composed of at least one three-component short-period seismometer. Three of them have four three-component geophones deployed in dedicated shallow wells down to 100 m. One station, VDH4, is composed of a broadband sensor, a velocimeter and an accelerometer and the associated data sent in real-time to the Observatoire Sismologique du Nord-Est de la France (ObS-NEF) hosted by the École et Observatoire des Sciences de la Terre (EOST) of the University of Strasbourg. Two other permanent stations also maintained by Fonroche are available and located about 10 km to the south-west.

In addition to the permanent network, KIT deployed end of 2018 - beginning of 2019, in the frame of the DEEPEGS project, a temporary network of four surface stations (VD1415, VD1416, VD1417, VD1419) in order to monitor the stimulation campaign of the VDH-GT2 well. The temporary stations installed at the west side of the developed zone improved the azimuthal coverage of the existing network. However, the vicinity of highways and main roads did not improve much the network detection sensitivity. In this urban area, selection of seismically quiet places was difficult and apart from station deployed at depth, the seismic background noise level often reached the "new high noise level" defined by Peterson (1993).

3.2 Data Processing

3.2.1 Monitoring System and Earthquake Detection

The monitoring system is based on the use of the open software Earthworm (EW) complemented by python scripts based on the open source seismological library ObsPy (Beyreuther *et al.* 2010). This entire automatic system is deployed on a virtual machine with linux OS and hosts:

1. a EW instance for real time acquisition and processing of data from the permanent network stations;

2. a EW instance for historical data playback to calibrate the geophysical parameters;
3. a MySQL database and a Winston Wave Server for waveform storage;
4. python scripts running continuously for data analysis, noise evaluation and coincidence triggering. This last uses a band-pass filtering between 5 and 45 Hz, STA and LTA windows of 1 s and 20 s respectively, an activating threshold of 2.5 ratio and a deactivating threshold of 1.7. A stack of the envelopes (Hilbert transform) of the three components is made and the triggering is performed on the stack. Three stations must trigger within the same timespan to send an alert;
5. quakeBot for monitoring events detected by RéNaSS;
6. and a Swarm instance to visualize stations and events in addition to the waveforms, as well as to perform manual post-processing of the events by picking P- an S-wave arrival times before location.

The temporary network data corresponding to the identified local earthquakes were later added to the processing procedure to increase the number of observations.

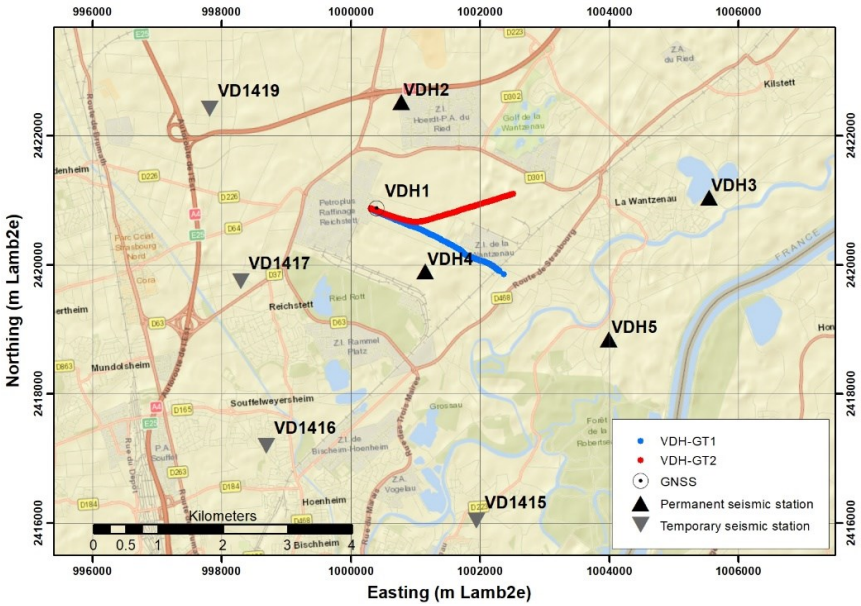

Figure 2: Map of the monitored area showing the trajectory of both wells of the doublet, VDH-GT1 (blue curve) and VDH-GT2 (red curve), the permanent seismic stations (black triangles) and the temporary stations (grey triangles).

3.2.2 Location and Magnitude Calculation

To locate the events, an initial 1D velocity model was built from the full sonic log performed in VDH-GT1. P- and S-wave velocities were averaged every 150 m along the log. For the first 130 m, no sonic data was available, therefore the first layer of the processed sonic was extended to the surface. At depth, the last layer of the processed sonic was extended to this sediment-basement interface, which was not logged, and the basement was given the velocity applied in the Rittershoffen geothermal field (Kinnaert *et al.* 2016). To account, to a certain extent, for the location sensitivity to the S-wave velocity model, the strongest induced earthquakes were located only with the P-waves and all time residuals, P and S, were used as stations corrections and systematically applied before locating all events. NonLinLoc software (Lomax *et al.* 2000; Lomax 2018) was used to locate the events.

Once located, an average local magnitude of the induced earthquake was calculated following the default approach of Bakun and Joyner (1984) but applied on the vertical component of the seismograms.

4. PRELIMINARY RESULTS AND DISCUSSION

4.1 Occurrence of Seismicity

Figure 3 shows the occurrence of the local seismicity and its magnitude induced by the hydraulic stimulation, which took place from 29/04/2019 20:30 to 16/05/2019 04:29. The detected and located seismicity was not felt and the estimated magnitude ranged between -0.6 and 1.2. Up to 14 events in 3 hours were identified. As observed, the seismicity is concentrated around two main periods, on the 5-6 May and on the 13-14 May 2019. The first seismicity appears about 6 days after stimulation started and ended about one day before it was stopped.

4.2 Seismicity Location

Figure 4 shows the location of the induced seismicity. As observed, the events are distributed in two unconnected clusters. The largest cluster is centered on the VDH-GT2 well within the 3.7 – 4.2 km depth interval. It contains the largest magnitude events that are located very close to the well. This depth range includes the open-hole section of the well that was stimulated hydraulically, the sediment-basement interface and the fault intersected by the well. Yet, it is not clear from the hypocenters whether this seismicity is associated with the shearing of this fault. The second cluster is approximately located 1 km deeper, between 4.7 and 5.2 km depth and it is not directly connected to the well. It only contains events with magnitude lower than 0.22.

According to the local geology, both clusters could belong to distinct NNE faults dipping west, but they could also belong to a single NNE antithetic fault. However, correlation of the event locations with structures identified by active seismic has to be further investigated.

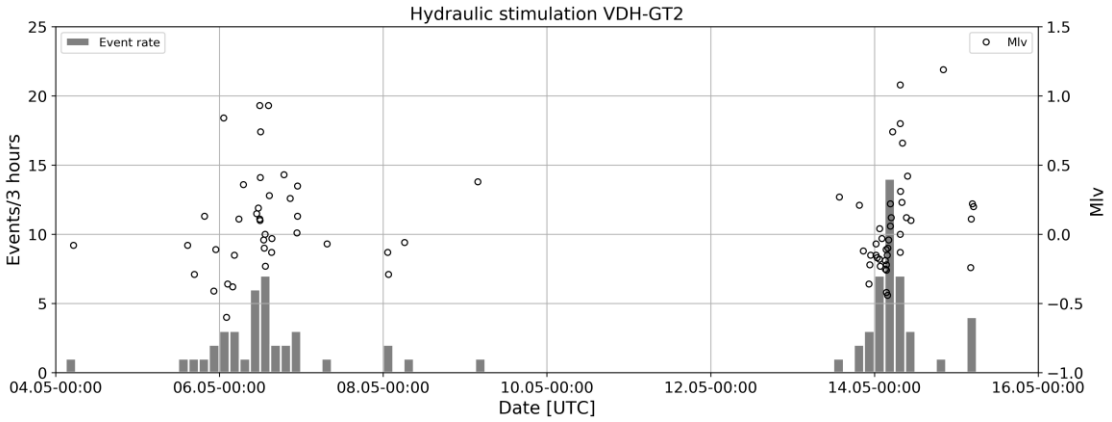

Figure 3: Occurrence of the seismicity induced during VDH-GT2 hydraulic stimulation. The seismic rate per 3 hours (grey bars) and the local magnitude (black points) are shown. The hydraulic stimulation started on 29/04/2019 at 20:30 and ended on 16/05/2019 at 04:29.

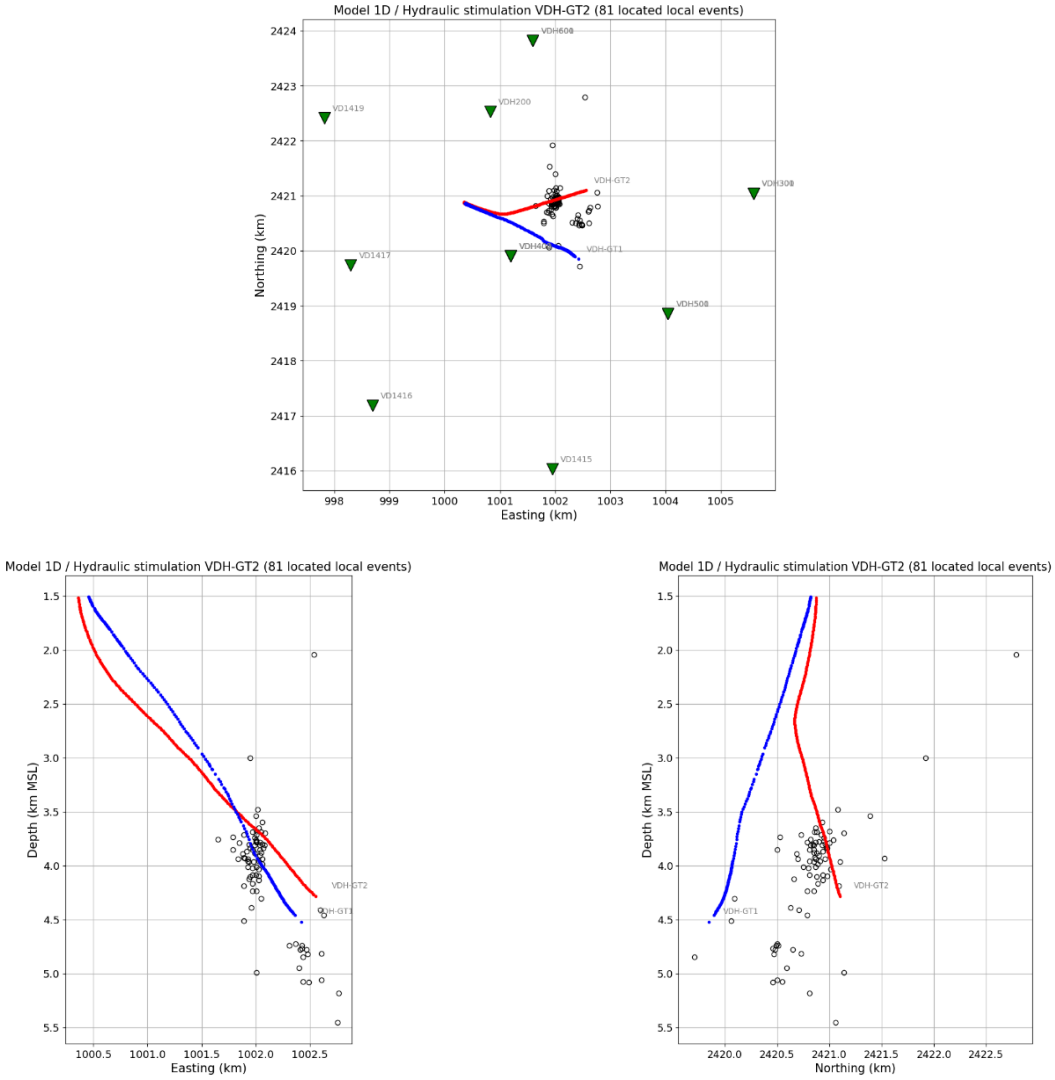

Figure 4: Hypocenter maps of the seismicity induced during VDH-GT2 hydraulic stimulation: plan view (top), vertical west-east projection (bottom left) and vertical south-north projection (bottom right).

4.3 Magnitude distribution

Despite the small number of recorded and located earthquakes, a magnitude of completeness was estimated at M_C=--0.35 (Figure 5). This shows that, despite the high concentration of seismic noise sources in the monitored area (highways, roads, railways, canals, shopping areas, cities) are relatively good sensitivity of the seismic network can be achieved. This threshold below M_L=0 is totally in accordance with the local monitoring regulations.

Assuming that the magnitude distribution follows a standard Gutenberg-Richter distribution, the b-value was estimated to 1.14 ± 0.02, which is slightly larger than the standard tectonic value of 1 and could be in accordance with higher values observed in EGS in the URG (Maurer *et al.* Submit.; Dorbath *et al.* 2009; Bachmann *et al.* 2011). However, the actual magnitude distribution is not perfect, in particular we can see a gap of magnitudes between 0.45 and 0.65. This is likely due to the small number of processed events, which limits the statistical analysis.

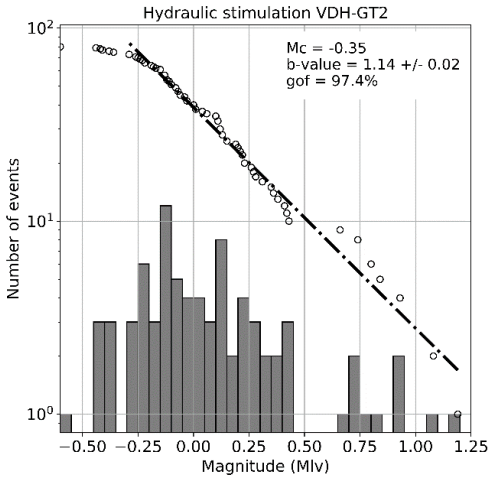

Figure 5: Frequency-magnitude distribution of the seismicity induced during VDH-GT2 hydraulic stimulation: cumulative number (black circles) and individuals events (gray histogram), and an estimate of the magnitude of completeness and b-values.

5. CONCLUSION

The hydraulic stimulation of the VDH-GT2 well induced unfelt seismicity, with local magnitude not exceeding 1.2. Preliminary location of the seismicity shows a distribution of hypocenters close to the well, at the sediment-basement interface and possibly in relation with the fault intersecting the well. The estimated b-value of 1.14 is slightly higher than standard tectonic context and may highlight the local effect of the hydraulic stimulation. Further data processing is however necessary to possibly increase the seismicity database and to better position the seismogenic underground structures of the geothermal reservoir.

REFERENCES

Bachmann C.E., Wiemer S., Woessner J. and Hainzl S. 2011. Statistical analysis of the induced Basel 2006 earthquake sequence: introducing a probability-based monitoring approach for Enhanced Geothermal Systems. *Geophysical Journal International* **186** (2), 793–807.

Bakun W.H. and Joyner W.B. 1984. The ML scale in central California. *Bulletin of the Seismological Society of America* **74** (5), 1827–1843.

Beyreuther M., Barsch R., Krischer L., Megies T., Behr Y. and Wassermann J. 2010. ObsPy: A Python Toolbox for Seismology. *Seismological Research Letters* **81** (3), 530–533.

Cornet F.H., Bérard T. and Bourouis S. 2007. How close to failure is a granite rock mass at a 5 km depth? *International Journal of Rock Mechanics and Mining Sciences and Geomechanics Abstracts* **44** (1), 47–66.

Delouis B., Haessler H., Cisternas A. and Rivera L. 1993. Stress tensor determination in France and neighbouring regions. *Crustal Stresses, Fractures, and Fault Zones: The Legacy of Jacques Angelier* **221** (3-4), 413–438.

Dèzes P., Schmid S.M. and Ziegler P.A. 2004. Evolution of the European Cenozoic Rift System: interaction of the Alpine and Pyrenean orogens with their foreland lithosphere. *Crustal Stresses, Fractures, and Fault Zones: The Legacy of Jacques Angelier* **389** (1-2), 1–33.

Dorbath L., Cuenot N., Genter A. and Frogneux M. 2009. Seismic response of the fractured and faulted granite of Soultz-sous-Forêts (France) to 5 km deep massive water injections. *Geophysical Journal International* **177** (2), 653–675.

Dorbath L., Evans K., Cuenot N., Valley B., Charléty J. and Frogneux M. 2010. The stress field at Soultz-sous-Forêts from focal mechanisms of induced seismic events: Cases of the wells GPK2 and GPK3. *Comptes Rendus Geoscience* **342** (7-8), 600–606.

Evans K.F., Zappone A., Kraft T., Deichmann N. and Moia F. 2012. A survey of the induced seismic responses to fluid injection in geothermal and CO2 reservoirs in Europe. *Geothermics* **41** (0), 30–54.

Friðleifsson G.Ó., Elders W.A., Zierenberg R.A., Stefánsson A., Fowler A.P.G., Weisenberger T.B., Harðarson B.S. and Mesfin K.G. 2017. The Iceland Deep Drilling Project 4.5 km deep well, IDDP-2, in the seawater-recharged Reykjanes geothermal field in SW Iceland has successfully reached its supercritical target. *Scientific Drilling* **23**, 1–12.

Kinnaert X., Gaucher E., Achauer U. and Kohl T. 2016. Modelling earthquake location errors at a reservoir scale: a case study in the Upper Rhine Graben. *Geophysical Journal International* **206**, 861–879.

Lomax A. 2018. The NonLinLoc home page. Available at: http://alomax.free.fr/nlloc/.

Lomax A., Virieux J., Volant P. and Berge-Thierry C. 2000. Probabilistic Earthquake Location in 3D and Layered Models. In: *Advances in Seismic Event Location*, Vol. 18 (ed. C. Thurber and N. Rabinowitz), pp. 101–134. Springer Netherlands. ISBN 978-90-481-5498-2.

Majer E.L., Baria R., Stark M., Oates S., Bommer J., Smith B. and Asanuma H. 2007. Induced seismicity associated with Enhanced Geothermal Systems. *Geothermics* **36** (3), 185–222.

Maurer V., Gaucher E., Grunberg M., Koepke R., Pestourie R. and Cuenot N. Submit. Seismicity induced during the development of the Rittershoffen geothermal field, France.

Meixner J., Schill E., Grimmer J.C., Gaucher E., Kohl T. and Klingler P. 2016. Structural control of geothermal reservoirs in extensional tectonic settings: An example from the Upper Rhine Graben. *Journal of Structural Geology* **82**, 1–15.

Peterson J.R. 1993. *Observations and modeling of seismic background noise.* U.S. Geological Survey.

Plenefisch T. and Bonjer K.P. 1997. The stress field in the Rhine Graben area inferred from earthquake focal mechanisms and estimation of frictional parameters. *Tectonophysics* **275** (1–3), 71–97.

Schumacher M.E. 2002. Upper Rhine Graben: Role of preexisting structures during rift evolution. *Tectonics* **21** (1), 6.

Zang A., Oye V., Jousset P., Deichmann N., Gritto R., McGarr A., Majer E. and Bruhn D. 2014. Analysis of induced seismicity in geothermal reservoirs – An overview. *Geothermics* **52**, 6–21.

Ziegler P.A. 1992. European Cenozoic rift system. *Tectonophysics* **208** (1–3), 91–111.

Acknowledgements

This work was carried out in the frame of the DEEPEGS Project, which is funded by the European Union's Horizon 2020 research and innovation programme under grant agreement No. 690771. We warmly thank R. Köpke, from KIT, who was strongly involved in the maintenance of the temporary seismic network of the KIT.